

Konrad-Zuse-Zentrum für Informationstechnik Berlin
Takustr. 7, D-14195 Berlin-Dahlem

P. Deuffhard* M. Seebass D. Stalling R. Beck H.-C. Hege

Hyperthermia Treatment Planning in Clinical Cancer Therapy: Modelling, Simulation, and Visualization

* Plenary keynote speaker, 15th IMACS World Congress 1997

Hyperthermia Treatment Planning in Clinical Cancer Therapy: Modelling, Simulation, and Visualization

P. Deuffhard M. Seebass D. Stalling R. Beck H.-C. Hege
e-mail: {deuffhard,seebass,stalling,beck,hege}@zib.de

Abstract

The speaker and his co-workers in *Scientific Computing and Visualization* have established a close cooperation with medical doctors at the Rudolf–Virchow–Klinikum of the Humboldt University in Berlin on the topic of *regional hyperthermia*. In order to permit a patient–specific treatment planning, a special software system (**HyperPlan**) has been developed.

A mathematical model of the clinical system (*radio frequency applicator with 8 antennas, water bolus, individual patient body*) involves Maxwell’s equations in inhomogeneous media and a so–called bio–heat transfer PDE describing the temperature distribution in the human body. The electromagnetic field and the thermal phenomena need to be computed at a speed suitable for the clinical environment. An individual geometric patient model is generated as a quite complicated tetrahedral “coarse” grid (several thousands of nodes). Both Maxwell’s equations and the bio–heat transfer equation are solved on that 3D–grid by means of *adaptive* multilevel finite element methods, which automatically refine the grid where necessary in view of the required accuracy. Finally optimal antenna parameters for the applicator are determined .

All steps of the planning process are supported by powerful *visualization* methods. Medical images, contours, grids, simulated electromagnetic fields and temperature distributions can be displayed in combination. A number of new algorithms and techniques had to be developed and implemented. Special emphasis has been put on advanced 3D interaction methods and user interface issues.

Keywords: cancer therapy planning, grid generation, patient model, Maxwell’s equations, heat transfer, visualization techniques, simulation environment

1 Introduction

Regional hyperthermia is a rather recent promising modality of cancer therapy based on the *local* heating of tumor tissue to about 44°C – usually applied *in combination with* radio- or chemotherapy. The aim is to optimize the generated temperature distribution within the patient’s body such that essentially the tumor is heated, but preferably *not* any sane tissue. For this reason, patient-specific treatment planning is necessary, which involves the segmentation of medical image data, the generation of geometrical patient models, and the solution of partial differential equations. We have developed an integrated software system (**HyperPlan**) from the scratch, where the entire process is backed by problem-specific visualization techniques. It allows the medical doctors to perform therapy planning in their clinical environment. In what follows we are going to describe main issues of mathematical modelling, numerical simulation and scientific visualization. Because of the restrictive space of this paper the important and challenging segmentation part of the task is omitted.

2 Modelling

As can be seen in the center of Fig. 1, the cancer affected region of a patient is surrounded by a so-called *applicator*, which essentially consists of (at present) eight radio frequency antennas (wavelength in water ca. 30 cm) and a water bolus to allow for a convenient passage of the radio waves into the body. The whole system is mathematically modelled by Maxwell’s equations in inhomogeneous media and a so-called bio-heat transfer partial differential equation describing the (time dependent) temperature distribution – see bottom frame in Fig. 1.

Electromagnetic Model. The antennas are driven with a fixed angular frequency ω . Initial transients can be neglected. As a simplification, the human tissues are modelled as linear isotropic charge-free media, so that Ohm’s law can be assumed. We are then left with Maxwell’s equations for time-harmonic fields in the form (**H**: magnetic field, **E**: electric field)

$$\text{curl } \mathbf{H} = i\omega\epsilon\mathbf{E}, \quad \text{curl } \mathbf{E} = -i\omega\mu\mathbf{H}, \quad (2.1)$$

where μ is the permeability and ϵ represents a complex dielectric function, related to the generic dielectric constant ϵ' and the conductivity σ by $\epsilon = \epsilon' - i\sigma/\omega$. The equations in (2.1) are combined to the well-known double-curl equation

$$\text{curl} \left(\frac{1}{\mu} \text{curl } \mathbf{E} \right) - \omega^2\epsilon\mathbf{E} = 0 \quad (2.2)$$

which will be the basis for our subsequent FE simulation.

Heat Transfer Model. Our present model for the dissipation of heat in the human body assumes *potential blood flow* within the various tissues including the tumor. This leads to the so-called *bio-heat transfer equation* (BHTE)

$$\rho_t c_t \frac{\partial T}{\partial t} = \text{div}(k \text{ grad } T) - W \rho_b \rho_t c_b (T - T_a) + Q, \quad Q = \frac{\sigma}{2} |\mathbf{E}|^2 \quad (2.3)$$

with ρ_t, ρ_b denoting the density of tissue and blood, c_t, c_b the specific heat of tissue and blood, T, T_a the temperature of tissue and arterial blood, k the thermal conductivity of tissue, W the blood perfusion, Q the power deposition within the tissue, and σ the electric conductivity. The thermal effects of *strong* arteria or veins are definitely excluded in this simplified model – but will be included in a future stage of the project. Moreover, *nonlinear* phenomena like systemic anticipation, which would essentially lead to nonlinear diffusion models, will also be studied later.

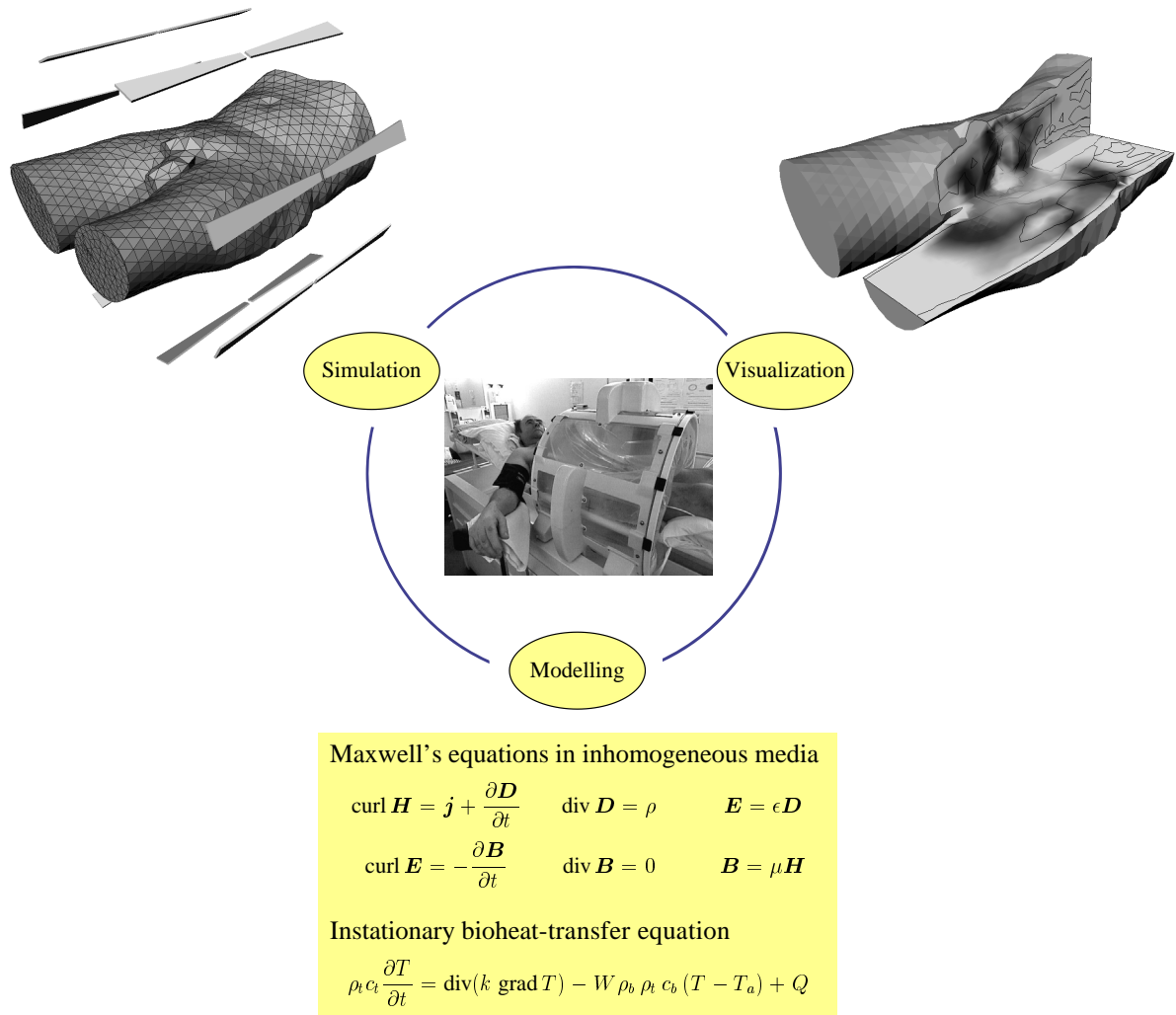


Figure 1: *Regional hyperthermia: necessary contributions for a patient specific treatment planning.*

Optimization. The genuine aim of hyperthermia treatment planning is to determine control parameters of the eight antennas in such a way that a favorable temperature distribution is achieved. Such a distribution can be characterized by the requirements that the heating should be concentrated in the tumor, and “hot spots” in healthy tissue should be avoided. Besides that the temperature in healthy tissue must not exceed certain temperature limits, which may depend on the tissue type.

As an associated mathematical model, we have chosen to *minimize* the objective function

$$q = \int_{\substack{r \in V_{tm} \\ T(r) < T_{th}}} (T_{th} - T(r))^2 dV + W_h \int_{\substack{r \notin V_{tm} \\ T(r) > T_h}} (T(r) - T_h)^2 dV \quad (2.4)$$

subject to box type constraints $T(r) \leq T_{lim}(r)$ which are applied for all $r \notin V_{tm}$. In these expressions V_{tm} denotes the tumor region, T_{th} the therapeutic temperature level, W_h a weighting factor for healthy tissue, T_h the temperature that should not be exceeded in healthy tissue, and $T_{lim}(r) \geq T_h$ the temperature limit, dependent on the tissue type at point r .

Model Validity. Of course, patient-specific material data would be necessary as input for our model equations. The presently available input data just originate from general experimental measurements [17, 12]. At least sensitivity studies or, even better, patient-specific measurements in the course of the treatment should be done. With all the indicated restrictions and simplifications, our simulation results on the basis of the described model are in surprisingly good agreement with clinical evidence. However, 3D modelling turned out to be inevitable, since previous 2D models had appeared to be insufficient.

3 Simulation

With the above partial differential equations (PDE's) given as mathematical model, the task is to simulate these PDE's for the complicated 3D geometry of patient and applicator. In order to allow for medical decisions based on the simulations, the applied computational methods must be robust and highly reliable. Moreover, to be feasible in clinical routine, the computations necessary for treatment planning should not consume more than a few minutes on a workstation. In this situation, *adaptive multilevel* (or multigrid) *methods* on a *finite element (FE) basis* are the methods of choice.

Basic Grid Generation. Any of the adaptive FE methods to be described below require an initial coarse grid, which captures the essential geometric features of the stated problem including a subdomain characterization for the different materials (bone, fat, muscle, ...). In view of the construction of *adaptive* grids for a complicated 3D geometry *tetrahedral elements* have been selected. In the coarse grid the elements should be nearly uniform within each tissue compartment. The total number of elements should be as large as necessary to state the problem correctly, but as small as possible in order to reduce computational costs.

During the past three years we have developed a new approach for grid generation, which avoids some drawbacks of the former "slice oriented" approach and significantly reduces the over-all time needed (see Table 1). Our present grid generator performs three steps:

- *Extraction of compartment interfaces from segmentation results.* For this purpose we have generalized the *marching cubes* algorithm [15] to non-binary classifications [10]. Similar as in the original algorithm, a significant speed-up is obtained via lookup-tables. The contributions of the basic cells are collected in *surface patches*, each separating two specific tissue compartments.
- *Remeshing the compartment surfaces.* In this step a coarsening of the surfaces is performed to allow for a basic grid with as few elements as possible. For remeshing we apply an *advancing front* method to each surface patch. Triangle sizes are adapted to surface curvature [19].
- *Tetrahedral mesh generation.* Each compartment is covered with tetrahedra starting from its surface using a *3D-advancing front* method. Such a method can be characterized by the strategies for selecting the next triangle of the front and for picking a suitable fourth point which completes the triangle to a tetrahedron. Concerning the first strategy our approach is similar to [11], but our second strategy has the advantage that a much smaller number of tetrahedra in question has to be tested [18].

The whole grid generation process can be performed automatically within 15 minutes CPU time on a UNIX workstation. An average coarse grid patient model generated as described consists of 30,000 - 40,000 tetrahedra and 6,000 - 7,000 vertices.

Adaptive Multigrid Maxwell Solver. In view of a FEM to be applied we start from the double-curl equation (2.2) for the electric field [1] and set up the functional

$$F(\mathbf{E}) = \frac{1}{2} \int \left\{ \frac{1}{\mu} (\operatorname{curl} \mathbf{E})(\operatorname{curl} \mathbf{E}) - \omega^2 \epsilon \mathbf{E} \mathbf{E} \right\} dV \quad (3.1)$$

which has to be stationary for the desired solution \mathbf{E} . Additional terms to account for problem-specific boundary conditions are neglected for ease of presentation.

In order to achieve a physically consistent modelling of the continuity relations for the electric field, we use finite elements based on Whitney-forms [4], which are equivalent to the H(curl)-conforming NÉDÉLEC elements of lowest order [16].

As is well-known, the curl-operator has an ample nullspace, which renders ill-conditioning of the linear systems to be solved numerically and severely impairs the convergence of any iterative solver of multilevel type. The finite element matrices arising in our problems are complex symmetric; the most promising candidate for a basic iterative solver was a conjugate residual algorithm. Nevertheless, the question of a good preconditioner still remains. In principle, Gauß-Seidel relaxation serves as an efficient smoother, but cannot cope with the modes of the nullspace. To improve this deficiency, we developed a projection scheme based on a Helmholtz decomposition of the discrete electric field [2]. Here the nullspace appears to be the gradient part of the field and may be represented within a space spanned by the gradients of Lagrange-type nodal basis functions. Now an additional smoothing step is carried out in the gradient space to attenuate the unwanted modes. This procedure accelerated the linear solver by a factor 4 already on the basic grid. In a multilevel setting with adaptively refined grids, the convergence rate of the solver remained independent of the number of refinement levels.

As we have to cope with strongly inhomogeneous materials and complex geometric structures, local mesh refinement is another important aspect with regard to reliability and efficiency. We developed an error estimator specifically tailored for Whitney-forms. It is based on stress-recovery [23], where the dual field variable \mathbf{H} , obtained by a simple derivation from the solution \mathbf{E} due to (2.1), is improved by an L_2 -projection into the Whitney basis [2].

As for the boundary conditions, the finite element mesh has been extended to a spherical region covering the complete arrangement of patient and antenna array. The ‘infinite’ space beyond this region is approximately taken into account by local absorbing boundary conditions [13] based on a radial field expansion. This type of boundary conditions preserves both symmetry and sparsity of the matrix.

Adaptive Multilevel Temperature Solver. The numerical solution of the (linear) bio-heat transfer equation (2.3) is by far less challenging than the just described Maxwell part. We apply the adaptive multilevel FEM from the toolbox KASKADE [6, 3, 1]. First numerical simulations for *nonlinear* diffusivity have been demonstrated in [9] and will be further pursued using the recently developed nonlinear elliptic solver NEWTON-KASKADE due to [7, 8].

Applicator Optimization. For optimization in the sense of (2.4) a *superposition principle* for temperature distributions is exploited. As long as heat transfer is modelled using the

linear BHTE (2.3), it is sufficient to perform temperature calculations for n^2 suitable sets of antenna parameters (with n the number of independent channels of the hyperthermia applicator). Then the temperature distribution for arbitrary antenna parameters can be determined very fast by superposition.

We apply a *damped Newton* method for minimizing the objective function (2.4), where the constraints are enforced by a penalty term. The result of an optimization is shown in Figure 2.

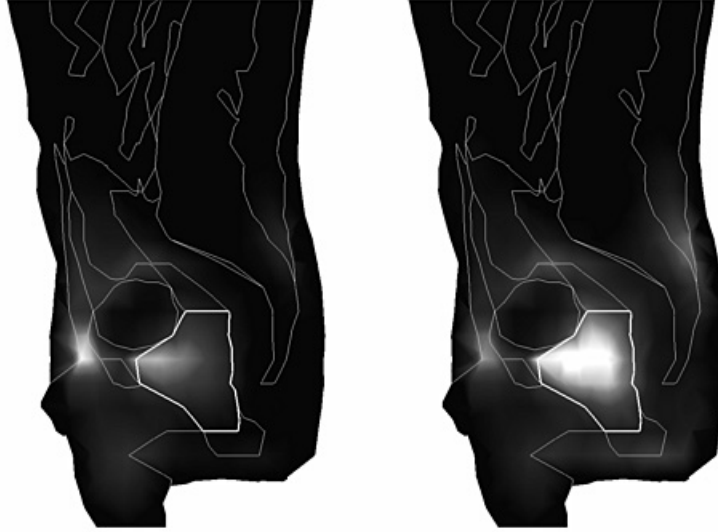


Figure 2: *Temperature distribution in a sagittal section of a patient model. Left: manually adjusted antenna parameters. Right: optimized antenna parameters. Note the increased heating of the tumor (accentuated by a bold white contour) and the diminished hot spot near the frontal surface of the body.*

Current Status. The effect of three years' work on the simulation part of the project is summarized in Table 1. As can be seen there, the '94 status was dominated by *interactive* work that required several days – as opposed to the '97 status, where such activities have been reduced to approximately 2 hours only. Most of the time is presently spent in the (still interactive) segmentation process and in the electric field computation, which therefore remain the two bottlenecks.

	initial status January '94	current status June '97
segmentation	interactive 2 days	interactive 2 hours
grid generation	interactive 2 days	automatic 15 minutes
field calculation	automatic 12 hours	automatic 80 minutes
temperature calculation	automatic 10 minutes	automatic 10 minutes
optimization	automatic 30 seconds	automatic 10 seconds
total	ca. 5 days	4 hours

Table 1: *Time required for patient-specific hyperthermia treatment planning.*

4 Visualization

Visualization and interaction techniques are important throughout the whole planning process. This includes both *data pre-processing*, i.e. segmentation and grid generation, as well as *data post-processing*, i.e., display and analysis of the simulation results. Therefore, to facilitate treatment planning in regional hyperthermia, we have developed the software system HyperPlan, which provides powerful methods from computer graphics and image processing and combines all simulation steps in an integrated environment [20].

Special care has been taken to create a robust and user-friendly system. At the same time HyperPlan is designed to be very flexible and easy to extend. This very combination makes it a valuable tool both in research and in clinical practice. Outside of ZIB, the system is currently being used at the Virchow-Klinikum in Berlin and at the Klinikum Großhadern in Munich.

Several data modalities are encountered during the planning process. In the following we describe some approved visualization methods for these modalities which are provided by HyperPlan. All methods can be applied in combination, too. This is an important feature which allows the therapist to assess the quality of a tetrahedral grid approximating the anatomy, to judge the dependence of calculated field distributions upon the underlying grid, or to detect tissue compartments affected by temperature hot spots.

Treatment Unit. Displaying geometric objects like the antennas or other parts of the applicator is often quite helpful. It enables the physician to recognize and adjust the position of the treatment units relative to the patient. Our system is based on the Open Inventor graphics toolkit. This toolkit defines a powerful data format for geometric objects which allows us to load and display any kind of external geometry.

Tomographic Images. Tomographic image data are most effectively analyzed by looking at 2D slices. HyperPlan can display slices of arbitrary orientation. Several methods are provided to map data to gray levels, e.g. a simple clamped linear mapping or a contrast-limited histogram equalization technique. To emphasize spatial relationships, the slices are usually displayed in a 3D window together with other geometric objects.

A more advanced method for visualizing tomographic image data is direct volume rendering. Though computationally very expensive, direct volume rendering can be implemented at interactive rates by exploiting the 3D-texture mapping capabilities offered by modern graphics workstations [5]. In addition to traditional volume rendering, HyperPlan also offers maximum intensity projections. This technique is especially useful for analyzing complex blood vessel structures.

Segmentation Results. In order to facilitate manual segmentation methods as well as to verify the results of automatic segmentation algorithms, special visualization techniques are required. The most simple approach is to draw contours on top of 2D tomographic images. Alternatively, particular regions in a 2D image may be highlighted using color or line patterns. More advanced methods are needed for understanding the shape of 3D-regions within a labelled volume. We have developed a method that allows the user to look at these regions using an ordinary cutting plane. Individual regions can then be selected and displayed in 3D by clicking onto the plane [22]. This kind of user interaction can also be used to control semi-automatic segmentation methods, e.g. volume growing or split-and-

merge algorithms.

Tetrahedral Patient Models. In order to visualize the structure of a tetrahedral patient model either tetrahedra of a particular tissue type may be displayed or boundary faces between neighbouring tissue compartments may be extracted. Several drawing styles are provided, including wire frames, shaded triangles, or triangles with superimposed edges. Superimposed edges are particularly helpful for understanding complex spatial geometries. To be able to render even large grids at interactive frame rates, acceleration strategies like polygon culling or ordered vertex traversal are being used.

Again, 3D-interaction techniques are provided to select tetrahedra for a more detailed inspection of the grid. In order to focus on certain areas of the grid, resizable boxes may be used. In addition, by clicking on triangles individual tetrahedra may be selected or removed. In this way the user may “carve out” a way to interesting interior grid structures.

Electromagnetic Fields. The fundamental quantities in radio frequency hyperthermia simulation are electromagnetic fields. In this respect methods for visualizing vector fields are of particular importance in our application. Beside the display of static fields, visualization of time-harmonic fields is necessary in order to reveal wave patterns and polarisation characteristics. In addition to a number of traditional “arrow style” methods, novel visualization techniques like line-integral convolution (LIC) have been incorporated into HyperPlan. As compared to traditional approaches, LIC is capable of encoding directional information at a much higher spatial resolution. This is illustrated in the left part of Fig. 3. An efficient algorithm (fastLIC) has been developed at ZIB which allows us to compute LIC images on 2D slices at acceptable rates [21].

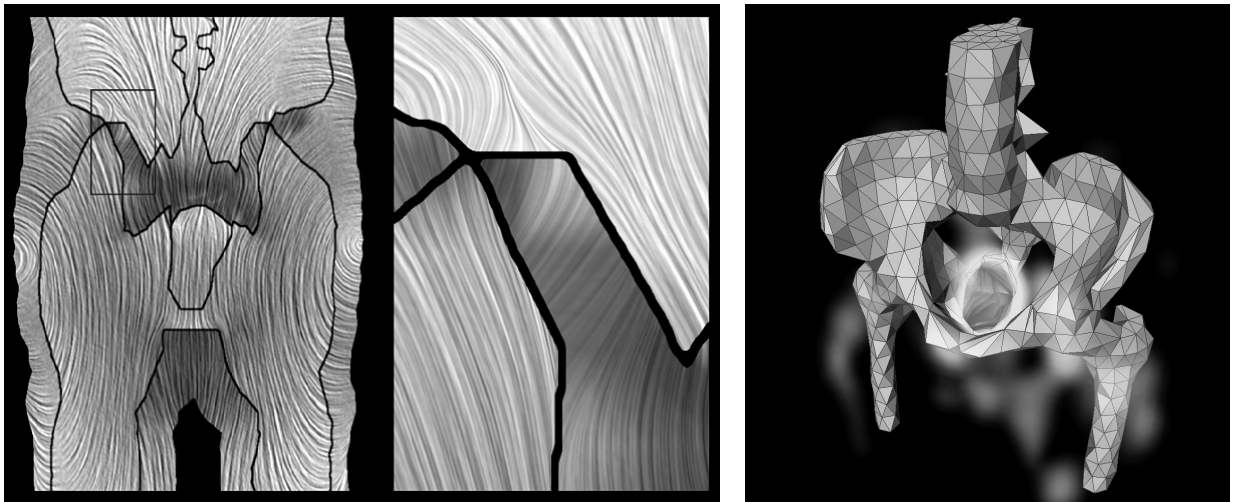


Figure 3: *LIC image of simulated electric field inside a patient (left). Parts of a patient grid together with volume rendered temperature distribution (right).*

Power and Temperature Distributions. Several different methods have been implemented to visualize scalar quantities defined on the tetrahedral grid, like simulated power or temperature. Among these methods are isolines, isosurfaces, arbitrarily oriented cutting planes, as well as a colorwash method, which displays scalar data on top of tomographic

images, thereby allowing the therapist to judge the data with respect to the anatomic situation. Moreover, we have developed a direct volume rendering method based on a cell-projection approach. Making use of hardware-accelerated texture mapping, the method can be applied to piecewise linear fields defined on a tetrahedral grid (cf. Fig. 3 right hand side).

In close cooperation with physicians, we aimed at achieving most meaningful visualization results by properly combining the methods described above. The main goal is to present diverse visual information in a single 3D scene, thus revealing insight into their interrelations. As in all medical applications special emphasis must be laid on the *reliability* of the displayed information. We tackle this problem by providing a set of tools for exact numerical data analysis, so-called *quantitative graphics tools*. They allow, for example, to query data values at arbitrary positions or to plot any scalar quantity along an arbitrary line segment.

Conclusion

Regional hyperthermia, a rather recent and promising modality of cancer therapy, has appeared to be a source of real challenges in *Scientific Computing and Visualization*. New adaptive multigrid algorithms for the numerical solution of the arising partial differential equations in complicated 3D geometries and new fast visualization algorithms for an intuitive visual representation of scalar and vector fields had to be designed. In close cooperation with medical doctors the integrated software system (HyperPlan, comprising approximately 200,000 lines of code) has been developed. In the near future a commercial version of this system will be sold together with the hyperthermia applicator BSD 2000. On this basis, an *individually* optimized therapy will be possible worldwide in clinical environments.

Acknowledgements: The authors gratefully acknowledge extremely fruitful cooperation with P. Wust, J. Nadobny, J. Gellermann from the Rudolf-Virchow-Klinikum (Abteilung für Radiologie, director: R. Felix), H. Oswald, S. Wegner from the Deutsches Herzzentrum Berlin (director: E. Fleck), and M. Zöckler (ZIB). This work has been supported by the Deutsche Forschungsgemeinschaft (DFG) within the Sonderforschungsbereich 273 “Hyperthermie: Methodik und Klinik”.

REFERENCES

- [1] R. Beck, B. Erdmann, R. Roitzsch: *An Object-Oriented Adaptive Finite Element Code and its Application in Hyperthermia Treatment Planning*, In: E. Arge, A. M. Bruaset, H. P. Langtangen, eds.: *Modern Software Tools for Scientific Computing*, Birkhäuser, 1997.
- [2] R. Beck, R. Hiptmair: *Multilevel Solution of the Time-Harmonic Maxwell's Equations based on Edge Elements*, Preprint SC-96-51, Konrad-Zuse-Zentrum für Informationstechnik Berlin, 1996.
- [3] F. Bornemann, B. Erdmann, R. Kornhuber, *Adaptive Multilevel-Methods in Three Space Dimensions*, *Int. J. Numer. Methods Eng.* 36, pp. 3187-3203, 1993.
- [4] A. Bossavit, *Whitney forms: a class of finite elements for three-dimensional computation in electromagnetism*, *Inst. Elec. Eng. Proc., Part A*, 135, No. 8, pp. 493-500, 1988.
- [5] B. Cabral, N. Cam, J. Foran, *Accelerated Volume Rendering and Tomographic Reconstruction Using Texture Mapping Hardware*, in *Proceedings of the IEEE Symposium on Volume Visualization '94*, pp. 91-98, 1994.
- [6] P. Deuffhard, P. Leinen, H. Yserentant, *Concepts of an Adaptive Hierarchical Finite Element Code*, *IMPACT Comput. Sci. Engrg.* 1, pp. 3-35, 1989.
- [7] P. Deuffhard, M. Weiser, *Local inexact Newton multilevel FEM for nonlinear elliptic problems*, Konrad-Zuse-Zentrum für Informationstechnik Berlin, Preprint SC 96-29, 1996. To appear in: *Proc. Comp. Science for the 21st Century*, Tours, France, May 1997.
- [8] P. Deuffhard, M. Weiser, *Global inexact Newton multilevel FEM for nonlinear elliptic problems*, Konrad-Zuse-Zentrum für Informationstechnik Berlin, Preprint SC 96-33, 1996. Invited paper, to appear in: W. Hackbusch, G. Wittum, (eds.), *Proc. 5th European Multigrid Conference (EMG '96)*, Springer, 1997.
- [9] B. Erdmann, J. Lang, M. Seebass, *Adaptive Solutions of Nonlinear Parabolic Equations with Application to Hyperthermia Treatments*, *Proc. Int. Symp. on Advances in Computational Heat Transfer*, Cesme, 1997.
- [10] H.-C. Hege, M. Seebaß, D. Stalling, M. Zöckler, *A Generalized Marching Cubes Algorithm Based On Non-Binary Classifications*, ZIB Preprint SC-97-05, 1997.
- [11] H. Jin, R. I. Tanner, *Generation of Unstructured Tetrahedral Meshes by Advancing Front Technique*, *Int. J. Numer. Methods Eng.* 36, pp. 1805-1823, 1993.
- [12] C. C. Johnson, A. W. Guy, *Nonionizing Electromagnetic Wave Effects in Biological Materials and Systems*, *Proc. IEEE* 60, pp. 692-718, 1972.
- [13] V.N. Kannelopoulos and J.P. Webb, *Numerical study of vector absorbing boundary conditions for the finite element solution of Maxwell's equations*, *IEEE Microw. Guided Wave Lett.* 1, pp. 325-327, 1991.
- [14] D. Laur, P. Hanrahan, *Hierarchical Splatting: A Progressive Refinement Algorithm for Volume Rendering*, *SIGGRAPH '91 Proceedings*, pp. 285-288, 1991.

- [15] W. E. Lorensen, H. E. Cline, *Marching Cubes: A high resolution 3D surface construction algorithm*, Computer Graphics 21:4, pp. 163-169, 1987.
- [16] J.C. Nedelec, *Mixed Finite Elements in R^3* , Numer. Math. 35, pp. 315-341, 1980.
- [17] H. P. Schwan, *Electrical Properties of Tissues and Cells*, Adv. Biol. Med. Phys. 5, pp. 147-209, 1957.
- [18] M. Seebass, D. Stalling, J. Nadobny, P. Wust, R. Felix, P. Deuffhard, *Three-Dimensional Finite Element Mesh Generation for Numerical Simulations of Hyperthermia Treatments*, Proc. 7th Int. Congress on Hyperthermic Oncology, Roma, Italy, April 1996, Vol. 2, pp. 547-548.
- [19] M. Seebass, D. Stalling, M. Zöckler, H.-C. Hege, P. Wust, R. Felix, P. Deuffhard, *Surface Mesh Generation for Numerical Simulations of Hyperthermia Treatments*, In: Proceedings of 16th Annual Meeting of the European Society for Hyperthermic Oncology, p. 146, Berlin 1997.
- [20] D. Stalling, H.C. Hege: *Design and Implementation of a Hyperthermia Treatment Planning System*, in B. Arnolds, H. Müller, D. Saupe, T. Tolxdorff (eds), Proc. of Workshop "Digitale Bildverarbeitung in der Medizin", Freiburg, March 9-10, 1995.
- [21] D. Stalling, H.C. Hege, *Fast and Resolution Independent Line Integral Convolution*, Proceedings of SIGGRAPH '95, (Los Angeles, California, August 6-11,1995). In *Computer Graphics Annual Conference Series*, ACM SIGGRAPH, pp. 249-256, 1995.
- [22] S. Wegner, D. Stalling, H.C. Hege, H. Oswald, E. Fleck, *Die 3D-Wasserscheiden-transformation auf Graphenebene – eine Anwendung für die Hyperthermieplanung*, in B. Arnolds, H. Müller, D. Saupe, T. Tolxdorff (eds), Proc. of Workshop "Digitale Bildverarbeitung in der Medizin", Freiburg, March 1997, pp. 31-36.
- [23] O. C. Zienkiewicz, J. Z. Zhu, *The superconvergent patch recovery (SPR) and adaptive finite element refinement*, Comp. Meth. Appl. Mech. Eng. 101, pp. 207-224, 1992.